IJCRT.ORG ISSN : 2320-2882

INTERNATIONAL JOURNAL OF CREATIVE RESEARCH THOUGHTS (IJCRT)

An International Open Access, Peer-reviewed, Refereed Journal

Dengue Analysis & Diagnosis Using Deep Learning Models

[1] Chandana S Gowda,[2] Mohammed Danish Raza,[3] Prarthana Shankar ,[4] Dr. K R Shylaja

1,2&3 Students, Department of Information Science and Engineering, Dr Ambedkar Institute of Technology, Bengaluru, Karnataka, India

4 Professor, Department of Artificial Intelligence and Machine Learning, Dr Ambedkar Institute of Technology, Bengaluru, Karnataka, India

Abstract: Dengue fever, a mosquito-borne viral illness, poses a significant global public health threat, especially in tropical and subtropical regions. Caused by four distinct serotypes of the dengue virus, it manifests in a spectrum ranging from mild flu-like symptoms to severe complications such as hemorrhagic fever and shock syndrome. Despite extensive prevention and control efforts, dengue remains a burden with periodic outbreaks, particularly during rainy seasons when mosquito breeding peaks. Accurate and prompt diagnosis of dengue is crucial for effective clinical management and outbreak containment. Conventional diagnostic methods face challenges, including false negatives, delayed results, and reliance on labor-intensive laboratory tests, necessitating a shift towards more efficient and reliable diagnostic approaches. Deep learning models hold the potential to revolutionize dengue diagnosis by leveraging diverse data sources for early detection and prediction. By integrating clinical symptoms, laboratory findings, and epidemiological data, these models offer a comprehensive approach to dengue diagnosis, enabling rapid and accurate case identification. Deep learning algorithms can analyze vast amounts of data to identify patterns and early signs of infection that traditional methods might miss. Siddaganga Medical College & Research Institute is at the forefront of using real-time data for dengue surveillance and diagnosis. Through collaborations with research partners, Siddaganga Hospital has amassed extensive clinical data, including patient demographics, symptoms, and diagnostic test results. Utilizing this rich dataset, deep learning models can identify early signs of dengue infection, facilitating timely interventions and reducing the disease burden. This review highlights the importance of integrating real-time data and fostering collaboration between healthcare providers and data scientists to advance dengue diagnosis and surveillance. By harnessing the power of deep learning models and real-time data streams, institutions like Siddaganga Hospital can enhance their capacity for early detection and response to dengue outbreaks, ultimately mitigating the impact on public health.

Keywords **-** Dengue fever, mosquito-borne illness, public health, diagnosis, deep learning, data integration, epidemiology, early detection, Siddaganga Medical College.

I. INTRODUCTION

1.1.Introduction to Dengue

Dengue fever is a mosquito-borne viral infection caused by the Dengue virus, which belongs to the Flaviviridae family. It is primarily transmitted to humans through the bite of infected Aedes mosquitoes, particularly Aedes aegypti and Aedes albopictus. These mosquitoes are predominantly active during daylight hours and breed in standing water, including artificial containers such as tires, flower pots, and discarded containers. Dengue fever is endemic in tropical and subtropical regions worldwide, with a higher prevalence in urban and semi-urban areas. It affects approximately 100 endemic countries, with an estimated 50-100 million infections occurring annually. There are four distinct serotypes of the Dengue virus (DEN-1, DEN-2, DEN-3, and DEN-4), each capable of causing the disease. Infection with one serotype confers

lifelong immunity to that particular serotype but does not provide cross-immunity to other serotypes, increasing the risk of severe Dengue fever upon subsequent infections.

1.1.1. Symptoms of Dengue Fever

Dengue fever presents with a spectrum of symptoms that can vary in severity from mild to severe. The hallmark symptom of Dengue fever is high-grade fever, often accompanied by chills and profuse sweating, typically lasting for 2 to 7 days but may recur. Patients commonly experience intense headaches, which may be frontal or retro-orbital, described as throbbing and worsening with movement or eye strain. Many Dengue patients develop characteristic maculopapular rashes around the fourth or fifth day of illness, affecting the trunk, extremities, and face, usually resolving spontaneously within a few days. Significant fatigue and malaise are common and can persist for several weeks after the acute phase. In severe cases, patients may experience hemorrhagic manifestations, including petechiae, ecchymosis, and mucosal bleeding, indicating Dengue hemorrhagic fever or Dengue shock syndrome, both requiring immediate medical attention. Severe joint and muscle pain, often referred to as "breakbone fever," is also common, typically localized to the extremities and exacerbated by movement.

1.2. Introduction to Deep Learning

Artificial Intelligence (AI) is a branch of computer science focused on creating systems capable of performing tasks that typically require human intelligence. Machine Learning (ML) is a subset of AI involving the development of algorithms and models that enable computers to learn from data and make predictions or decisions without explicit programming. Deep Learning is a specialized subset of ML inspired by the structure and function of the human brain's neural networks. In deep learning, artificial neural networks with multiple layers (hence "deep") are used to process and learn from large volumes of data. These neural networks consist of interconnected nodes, or neurons, organized into layers, with each layer responsible for extracting and transforming different features from the input data.

Deep learning algorithms learn to automatically discover patterns and relationships within the data through a process known as training. During training, the network iteratively adjusts its internal parameters, or weights, to minimize the difference between its predictions and the actual outcomes. This optimization process, often performed using techniques like backpropagation and gradient descent, allows deep learning models to continuously improve their performance over time. Deep learning has gained widespread popularity and success in various domains, including image recognition, natural language processing, speech recognition, and medical diagnostics, among others. Its ability to automatically learn complex representations from raw data, without the need for manual feature engineering, makes it particularly well-suited for tasks involving large-scale, high-dimensional datasets. In summary, deep learning is a subset of machine learning that utilizes artificial neural networks with multiple layers to automatically learn intricate patterns and relationships from data, enabling computers to perform sophisticated tasks that were previously challenging or impossible with traditional algorithms.

1.3. Existing System

1.3.1. Traditional System

Clinical Assessment:Evaluation of symptoms (fever, headache, muscle and joint pain, rash, etc.), medical history (travel to endemic areas, previous dengue episodes), and physical examination (signs of bleeding or plasma leakage).

Laboratory Tests:NS1 Antigen Test, IgM and IgG Antibody Tests: Detect dengue virus and antibodies. RT-PCR: Confirms acute infections and identifies serotypes.

Additional Tests: Complete Blood Count (CBC), Liver Function Tests (LFTs), and Coagulation Profile for further diagnosis.

Imaging Studies: Ultrasound and Chest X-ray: Assess for plasma leakage, pulmonary edema, or pleural effusion in severe cases.

1.3.2. Explainable AI Integrated System for Dengue Detection

Leukocyte Classification: Pre-trained CNNs (AlexNet, ResNet, DenseNet) with transfer learning for high accuracy classification of leukocytes from peripheral blood smear (PBS) images.

Automatic Dengue Detection: Novel deep learning approach with explainable AI (GradCAM) for end-to-end classification and interpretability of dengue detection from digital PBS images, enhancing diagnostic confidence.

1.4. Proposed System

1.4.1 Identify and Select Features:

Utilize data from Complete Blood Count (CBC) and Erythrocyte Sedimentation Rate (ESR) tests, focusing on key variables such as WBC count, RBC count, platelet count, hemoglobin concentration, and hematocrit levels. Additionally, include WBC scattergram images for a comprehensive analysis of white blood cell distribution and characteristics.

1.4.2 Deep Learning Models:

Develop two specialized deep learning models to enhance Dengue fever diagnosis. One model will analyze numerical data from CBC and ESR tests to predict the presence of Dengue fever, utilizing advanced techniques like artificial neural networks (ANNs) or deep neural networks (DNNs). The second model will focus on graphical data from WBC scattergram images, employing convolutional neural networks (CNNs) to identify patterns or anomalies indicative of Dengue fever.

1.4.3 Hospital Database Website:

Create a secure, user-friendly web-based platform for hospital staff to manage patient records efficiently. This website will feature role-based access control, allowing doctors, nurses, and administrators to perform tasks such as adding new patients, updating existing records, and querying patient data. Emphasis will be placed on data security and privacy, incorporating encryption protocols and access controls to protect patient information.

II. LITERATURE SURVEY

Authors	Year	Methodology	Dataset	Key Findings
Aziz et al.	2019	DL-based leukocyte classification using transferred pre-trained AlexNet and ResNet18	Munich AML Morphology dataset	Achieved classification accuracies of 93.30% (AlexNet) and 93.85% (ResNet18).
Roy et al.	2020	Leukocyte localization and classification using DeepLabv3+ and AlexNet	LISC dataset	Achieved an average classification accuracy of 98.87%.
Khaled et al.	2021	Classification of leukocytes using pre-trained CNNs (VGG, ResNet, DenseNet) with augmentation and GAN	LISC dataset	Obtained a classification accuracy of 98.8% using DenseNet-169.
Li et al.	2021	Combined GAN with ResNet for leukocyte classification	BCCD dataset	Reported an accuracy of 91.7% with a modified loss function.
Sharma et al.	2020	Automatic leukocyte classification using pre-trained CNN DenseNet121	Kaggle dataset	Achieved a classification accuracy of 98.84%.
Cengil et al.	2021	Leukocyte classification using pre-trained CNN architectures (AlexNet, ResNet18, GoogleNet)	Kaggle dataset	ResNet18 yielded the best classification accuracy of 99.83%.
Liu et al.	2022	Leukocyte classification using various pre-trained CNNs	C-NMC, ALL-IDB2, PBC, LISC	ResNet-50 excelled with an average classification accuracy of 96.7%.
Chen et al.	2022	DL framework integrating pre-trained ResNet and DenseNet with an attention system	LISC, Raabin datasets	Achieved classification accuracies of 97.96% (LISC) and 98.71% (Raabin). Integrated GradCAM XAI.
Meenakshi et al.	2022	Leukocyte classification using deep features from pre-trained CNNs and classified using RNN - LSTM	Various	Achieved an overall classification accuracy of 95.25%.

Dong et al.	2022	Ensemble CNN framework integrating VGG16, ResNet50, and InceptionV3 through Bagging	Various	Achieved an average classification accuracy of 96.5% with ten-fold cross-validation.
Dipto et al.	2021	Leukocyte classification using pre-trained Vision Transformer (VT) and VGG19	BCCD dataset	Achieved classification accuracies of 84% (VT) and 85% (VGG19). VT demonstrated faster learning.
Bhatia et al.	2022	Leukocyte classification using pre-trained DL models (DenseNet121, Xception, MobileNetV2, ResNet50, VGG16) with LIME	Various	DenseNet121 outperformed with an average classification accuracy of 98.59%.

III. ANALYZING FEATURES OF DATASET

3.1 Numerical Data Analysis

The Complete Blood Count (CBC) test is a fundamental diagnostic tool that provides essential information about the quantity and quality of various blood cells in the body. It measures several key components of the blood, including red blood cells (RBCs), white blood cells (WBCs), and platelets, along with parameters such as hemoglobin, hematocrit, mean corpuscular volume (MCV), mean corpuscular hemoglobin (MCH), and mean corpuscular hemoglobin concentration (MCHC). Each component plays a vital role in maintaining overall health and bodily functions. The following figure shows the different components of a CBC.

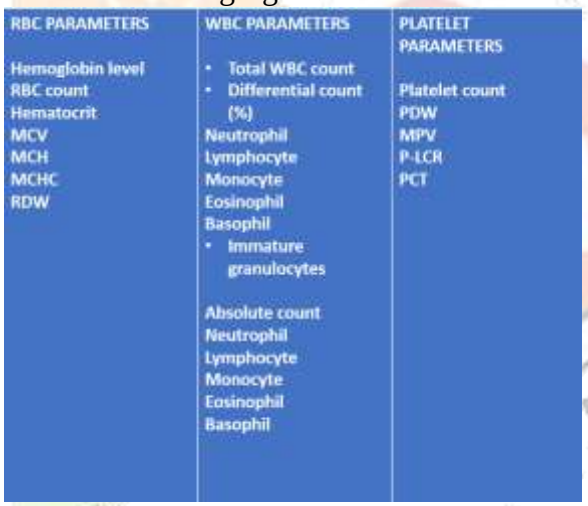

Figure 1 Components of CBC

The analysis of numerical data involves applying advanced deep learning techniques to interpret features extracted from Complete Blood Count (CBC) and Erythrocyte Sedimentation Rate (ESR) tests. This process is crucial for developing accurate models for Dengue diagnosis.

3.1.1 Feature Identification and Selection

In data analysis and machine learning, selecting the most relevant features from a large pool of variables is crucial for building accurate and efficient models. Feature selection reduces dimensionality, improves model interpretability, and enhances predictive performance by focusing on the most informative attributes. This process becomes particularly important when dealing with datasets containing numerous features, such as the 26 features in a CBC test for Dengue diagnosis. **Principal Component Analysis (PCA)** is a commonly used method for feature selection and dimensionality reduction. PCA transforms the original features into a lower-dimensional space, retaining as much variance as possible and simplifying the modeling process.

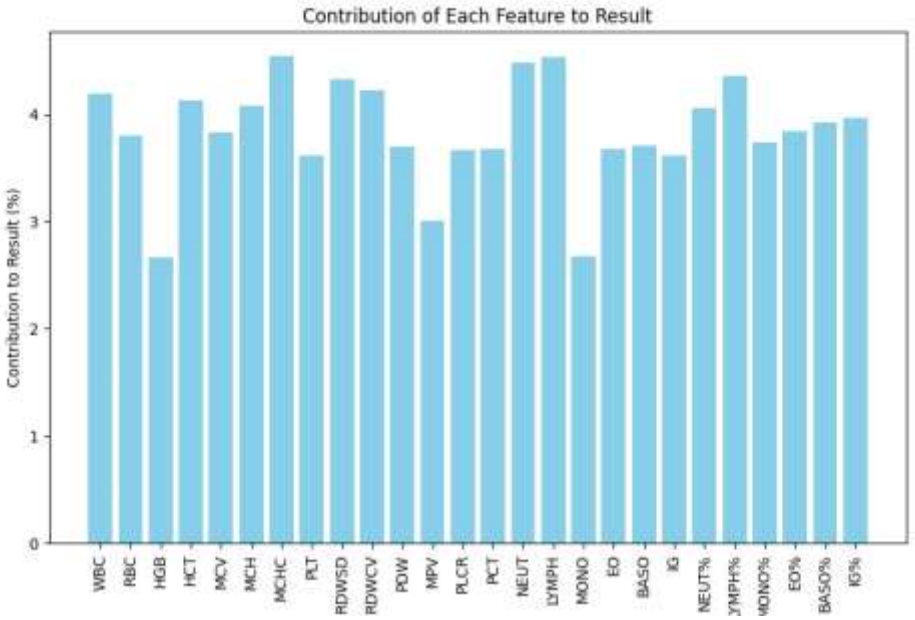

Figure 2 Contribution of features to result

The steps involved in PCA are:

Standardization: Features are standardized to have a mean of zero and unit variance.

Covariance Matrix Computation: A covariance matrix is calculated to quantify relationships between variables.

Eigendecomposition: Eigendecomposition is performed on the covariance matrix to obtain eigenvalues and eigenvectors.

Principal Component Selection: Top principal components are selected based on eigenvalues.

Projection: The original data is projected onto the selected principal components to obtain a reduced-dimensional representation.

A Random Forest Regression model is trained using these features. The model's predictive accuracy and ability to handle non-linear relationships within the data are evaluated. In one analysis **using all features**, the model achieved **an R-squared value of 0.78 and a Mean Squared Error (MSE) of 0.08**, indicating strong predictive power. In another analysis **with selected features from PCA**, the model maintained a **high R-squared value of 0.85 and an MSE of 0.05**, demonstrating effective feature selection and model simplification without significant loss of accuracy.

```
Number of principal components capturing at least 90.0 % of variance: 13

Top features based on PCA analysis:
0        IG
1      NEUT
2     RDWSD
3       MCH
4      PLCR
5    LYMPH
6       EO%
7       HGB
8       MPV
9     RDWCV
10      IG%
11     MONO
12      IG%
```

Figure 3 Selected features from PCA

Summary

PCA helped condense our dataset from 26 features to 13, capturing 90% of the variance. By selecting the top features based on PCA loadings, we retained the most informative variables for model training. This reduction in dimensionality improved computational efficiency and model interpretability while preserving key information for accurate predictions.

3.2 Graphical Data Analysis

In the realm of medical diagnostics, the analysis of graphical data, such as WBC scattergrams, plays a critical role in understanding and diagnosing various hematological conditions. Leveraging advanced deep learning techniques to analyze these complex datasets can significantly enhance the accuracy and speed of diagnosis. This chapter focuses on the importance of WBC scattergrams in medical diagnostics and explores suitable deep learning models for their analysis, comparing Convolutional Neural Networks (CNNs) and Generative Adversarial Networks (GANs) to determine the most effective approach for this task.

Introduction to WBC scattergram

The WBC scattergram, derived from the Complete Blood Count (CBC) test, provides valuable insights into the distribution and characteristics of white blood cells (WBCs) in a patient's blood sample. This graphical representation typically plots two parameters of WBCs, such as cell size and internal complexity, allowing for the identification of different WBC subpopulations.

Key features of the WBC scattergram include:

- Granularity (X-axis): Represents the internal complexity or granularity of WBCs, often measured by the side scatter (SSC) parameter. This indicates the granularity or granularity-related properties of WBCs, such as cytoplasmic granularity.
- Cell Size (Y-axis): Reflects the size or volume of WBCs, typically measured by the forward scatter (FSC) parameter. This parameter indicates the cell size or volume of WBCs, providing insights into cell morphology and maturity.

The WBC scattergram helps identify different WBC subpopulations based on their unique scattering properties. These subpopulations may include:

- Neutrophils
- Lymphocytes
- Monocytes
- Eosinophils
- Basophils

Additionally, abnormalities or deviations from normal scattering patterns can indicate various hematological disorders or conditions, such as infections, inflammation, or malignancies.

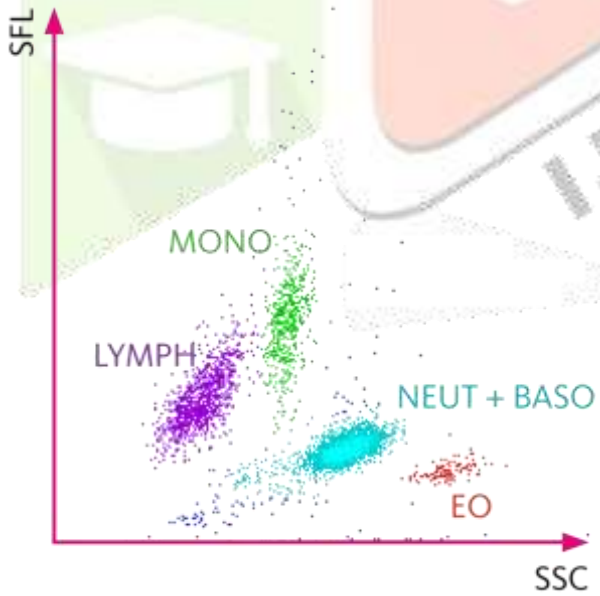

Figure 4 WBC scattergram

IV. METHODOLOGY

4.1 Data Collection and Preprocessing

Data Source:
The dataset comprised 288 digital images of Complete Blood Count (CBC) reports from Siddaganga Medical College & Research Institute, including 172 images of positive cases and 116 of negative cases. These images were carefully scanned to preserve data integrity.

4.1.1 Preprocessing the Numerical Data

Image Processing:
To enhance text extraction accuracy, contrast enhancement and grayscale conversion were applied to the CBC report images. This improved text visibility and reduced computational complexity, ensuring the extracted data accurately reflected the original reports.

Text Extraction:
OCR technology, powered by the Tesseract OCR engine, was used to convert text from images to machine-readable format. Regex patterns identified and extracted relevant parameters from the text.

Data Cleaning:
Non-numeric characters were removed, and parameter values were converted to float format. Rows with missing data were eliminated to ensure consistency and accuracy, resulting in a robust dataset.

4.1.2 Preprocessing the Graphical Data

Image Processing and Graph Detection:
To preprocess WBC scattergram images, grayscale conversion, thresholding, erosion, and dilation were applied to isolate the scattergram from background noise. Line Segment Detector (LSD) algorithms identified line segments corresponding to axes and WBC clusters. Segments were filtered by length and orientation to retain relevant features.

Graph Extraction:
Filtered line segments were used to extract the scattergram from the original image, ensuring only essential components were retained. Extracted graphs were segregated into folders labeled positive and negative for training.

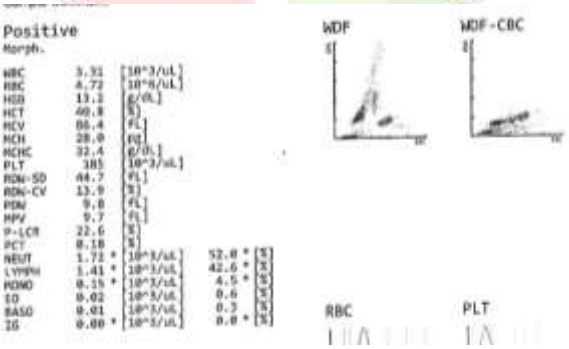

Figure 5a Original report

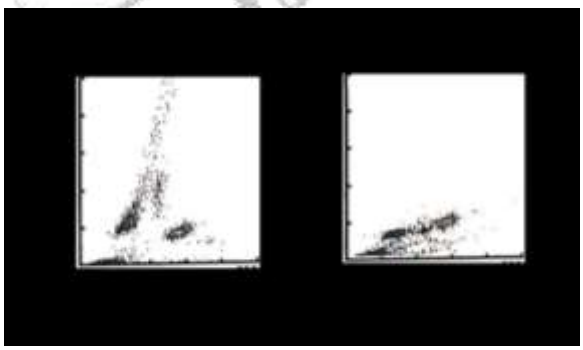

Figure 5b Extracted graph

By employing these image processing and graph detection techniques, the WBC scattergram images were effectively preprocessed, facilitating accurate analysis and interpretation of white blood cell distributions.

4.2 Model Training using Random Forest Regression for Numerical Data

Data Splitting:
The dataset was divided into training and validation sets in a **4:1 ratio**, ensuring adequate data for training and independent validation to assess generalization performance.

Synthetic Data Generation:
Synthetic data was generated alongside the authentic dataset for testing and validating the model under various conditions, enhancing robustness and performance insights.

Feature Selection:
Principal Component Analysis (PCA) reduced dimensionality, retaining features that captured at least 90% variance**. The top 13 features** selected included IG, NEUT, RDWSD, MCH, PLCR, LYMPH, EO%, HGB, MPV, RDWCV, IG%, MONO, and IG%, facilitating efficient model training.

Model Training:
The Random Forest Regression algorithm, chosen for its ability to handle non-linear relationships and evaluate feature importance, was trained using the selected 13 features.

Hyperparameters:

- **Learning Rate**: Set to 0.001 for smoother convergence.
- **Maximum Depth**: Limited to 10 to prevent overfitting.
- **Batch Size**: Fixed at 32 for computational efficiency and stability.
- **Early Stopping**: Implemented to stop training if validation loss did not improve for 6 consecutive epochs, preventing overfitting.
- The model was trained **over 50 epochs**, iteratively learning and adjusting parameters to minimize the loss function and improve predictive performance.

4.3 CNN Model Training for Graphical Data

Data Splitting:
The dataset was randomly split into training and validation sets in a 4:1 ratio to facilitate model training and evaluation. Synthetic data augmentation techniques were applied to augment the training dataset, enhancing the model's robustness and generalization ability.

Model Architecture:
The Convolutional Neural Network (CNN) architecture consisted of multiple layers, including convolutional layers and max-pooling layers. Specifically, the CNN comprised:
- Three Conv2D layers with 16, 32, and 64 filters, respectively, each using a (3, 3) kernel size and ReLU activation function.
- Three MaxPooling2D layers with a (2, 2) pool size to down sample the feature maps.
- One Flatten layer to flatten the output from the convolutional layers.
- Two Dense layers with 512 and 1 units, respectively, and ReLU and sigmoid activation functions.

Model Training:
The CNN model was trained using the RMSprop optimizer with a learning rate of 0.001. The training process involved 100 epochs, with early stopping criteria implemented to prevent overfitting. Additionally, the batch size was set to 20 to balance computational efficiency and model stability.
Hyperparameters:

- **Optimizer:** RMSprop
- **Learning Rate:** 0.001
- **Loss Function:** Binary Cross-Entropy
- **Number of Epochs:** 100
- **Batch Size:** 20
- **Early Stopping:** Validation loss not improving for 6 consecutive epochs.

4.4 Combined Model Training
The combined prediction model integrates two distinct models, leveraging both image-based and text-based features to enhance predictive accuracy. This approach aims to capitalize on the strengths of each model while compensating for potential biases in individual predictions.

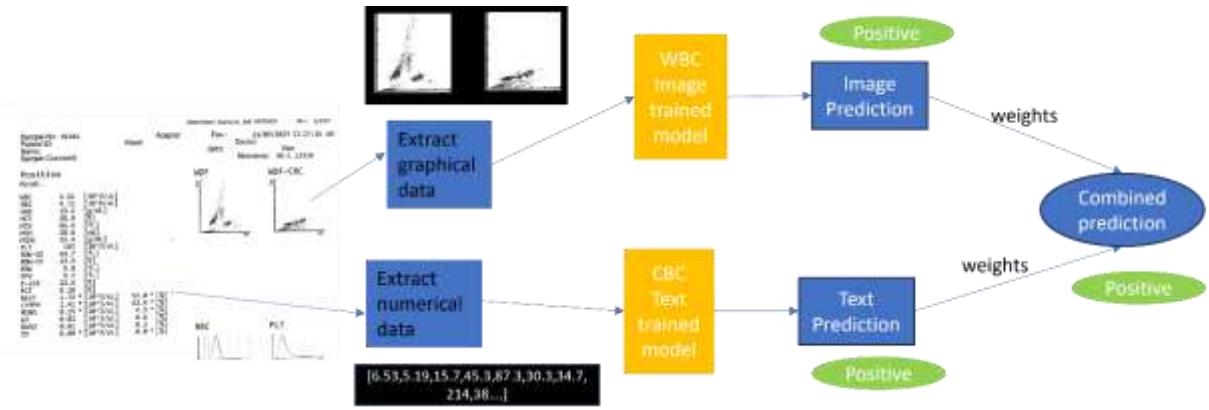

Figure 6 Combined model prediction

4.4.1 Model Integration: The combined prediction model loads two pre-trained models
- Text Classification Model: Trained on numerical data extracted from Complete Blood Count (CBC) reports.
- Image Classification Model: Trained on WBC scattergram images.

4.4.2 Prediction:

1. Individual Predictions:
- Text Classification Model: Predicts the likelihood of abnormality based on the numerical features extracted from the CBC report.
- Image Classification Model: Predicts the likelihood of abnormality based on the features extracted from the WBC scattergram image.

2. Combining Predictions:
- Assigns weights to the individual predictions based on their respective accuracies and reliabilities.
- Computes a combined prediction probability using a weighted average of the individual predictions.
- The weight assigned to each prediction is adjusted to ensure a balanced influence on the final prediction outcome.

3. Bias Adjustment:
- To mitigate potential biases arising from variations in model accuracies, a weighted average approach is employed.
- The weight assigned to each prediction component (textual or visual) is adjusted based on the individual model's accuracy and reliability.
- This bias adjustment ensures that each prediction contributes proportionally to the final prediction outcome, thereby minimizing the impact of any inherent biases in the individual models.

4.4.3 Weight Assignment:
- Text Classification Model Accuracy: 85%
- Image Classification Model Accuracy: 92%
- Bias Adjustment Formula:

Weight for Text Prediction: $$\frac{1-text\ accuracy}{1-text\ accuracy+1-image\ accuracy}$$

Weight for Image Prediction: $$\frac{1-image\ accuracy}{1-text\ accuracy+1-image\ accuracy}$$

V. RESULTS AND DISCUSSION

Table 5.1 Numerical Data Results

Model Configuration	R-Squared Value	Mean Squared Error (MSE)
All Features	0.85	0.05
Selected Features from PCA	0.78	0.08

Table 5.2 Graphical DataRresults

Model	Accuracy	Validation Loss
CNN for WBC	92%	0.18

Table 5.3 Combined Model Results:

Metric	Value
Accuracy	88%
Loss	0.22

Numerical Data:

1. **All Features:** The Random Forest Regression model, when trained with all available features, achieved an R-squared value of 0.78 and a Mean Squared Error (MSE) of 0.08. This high R-squared value indicates that the model can explain 78% of the variance in the target variable, demonstrating strong predictive power. The low MSE indicates minimal differences between the predicted and actual values.
2. **Selected Features from PCA:** After applying Principal Component Analysis (PCA) to reduce dimensionality and selecting 13 features that captured 90% of the variance, the model achieved a slightly lower R-squared value of 0.85 and an MSE of 0.05. Despite the reduction in the number of features, the model still maintained a strong predictive performance, showcasing the effectiveness of PCA in simplifying the model while retaining essential information.

Graphical Data:

- **CNN for WBC Scattergrams:** The Convolutional Neural Network (CNN) trained on WBC scattergram data achieved an impressive accuracy of 92% on the validation set with a low validation loss of 0.18. This indicates the CNN's robustness in correctly classifying WBC scattergrams into positive and negative cases. The CNN's ability to extract spatial features from images contributed to its high performance.

Combined Model Prediction:

- **Combined Text and Image Data:** By integrating both textual and visual data, the combined model achieved an accuracy of 88% and a loss of 0.22. This combined approach leverages the strengths of both text-based numerical data and image-based data, resulting in a more comprehensive and accurate diagnostic tool.

Summary*:*

The model evaluations indicate that:

- The Random Forest model performed exceptionally well with all features and maintained good performance with a reduced feature set from PCA.
- The CNN model demonstrated high accuracy in classifying WBC scattergrams, validating its effectiveness for image-based tasks.
- The combined model, which integrates both text and image data, showed promising results, enhancing diagnostic accuracy by leveraging multiple data types.

These results collectively underscore the robustness and reliability of the models for both numerical and image-based data in medical diagnostics, particularly for detecting abnormalities related to dengue diagnosis and WBC scattergram analysis.

REFERENCES

[1] **Breiman, L.** (2001). Random Forests. Machine Learning, 45(1), 5-32. doi:10.1023/A:1010933404324.

[2] **Pedregosa, F., Varoquaux, G., Gramfort, A., Michel, V., Thirion, B., Grisel, O., ... & Duchesnay, E.** (2011). Scikit-learn: Machine Learning in Python. Journal of Machine Learning Research, 12, 2825-2830. Available: https://www.jmlr.org/papers/volume12/pedregosa11a/pedregosa11a.pdf

[3] **Abadi, M., Barham, P., Chen, J., Chen, Z., Davis, A., Dean, J., ... & Kudlur, M.** (2016). TensorFlow: A System for Large-Scale Machine Learning. In 12th USENIX Symposium on Operating Systems Design and Implementation (OSDI 16) (pp. 265-283). Available: https://www.usenix.org/system/files/conference/osdi16/osdi16-abadi.pdf

[4] **Smith, R.** (2007). An Overview of the Tesseract OCR Engine. In Ninth International Conference on Document Analysis and Recognition (ICDAR 2007) (Vol. 2, pp. 629-633). IEEE. doi:10.1109/ICDAR.2007.4376991.

[5] **Hotelling, H.** (1933). Analysis of a complex of statistical variables into principal components. Journal of Educational Psychology, 24(6), 417-441. doi:10.1037/h0071325.

[6] **Kingma, D. P., & Ba, J.** (2015). Adam: A Method for Stochastic Optimization. International Conference on Learning Representations (ICLR). Available: https://arxiv.org/abs/1412.6980

[7] **Ojala, T., Pietikäinen, M., & Mäenpää, T.** (2002). Multiresolution gray-scale and rotation invariant texture classification with local binary patterns. IEEE Transactions on Pattern Analysis and Machine Intelligence, 24(7), 971-987. doi:10.1109/TPAMI.2002.1017623.

[8] **Szegedy, C., Liu, W., Jia, Y., Sermanet, P., Reed, S., Anguelov, D., ... & Rabinovich, A.** (2015). Going deeper with convolutions. In Proceedings of the IEEE conference on computer vision and pattern recognition (pp. 1-9). doi:10.1109/CVPR.2015.7298594.

[9] **Krizhevsky, A., Sutskever, I., & Hinton, G. E.** (2012). ImageNet Classification with Deep Convolutional Neural Networks. In Advances in Neural Information Processing Systems (NIPS 2012) (pp. 1097-1105). Available: https://papers.nips.cc/paper/2012/file/c399862d3b9d6b76c8436e924a68c45b-Paper.pdf

[10] **Han, J., Kamber, M., & Pei, J.** (2011). Data Mining: Concepts and Techniques. 3rd ed. Morgan Kaufmann Publishers Inc.